

Ultrasonography of the pancreas.

1. Conventional imaging

A. Martínez-Noguera,¹ M. D'Onofrio²

¹Department of Radiology, Hospital Sant Pau, Autonomous University of Barcelona, Sant Antoni M. Claret 167, 08025 Barcelona, Spain

²Department of Radiology, Policlinico G. B. Rossi, University of Verona, Piazzale L. A. Scuro 10, 37134 Verona, Italy

Abstract

Ultrasound imaging has made significant advances in recent years and plays an important role in the detection, characterization and staging of pancreatic diseases. Conventional ultrasonography (US) is a noninvasive imaging modality, which continues to be the first diagnostic step in the evaluation of the pancreas. Over its various decades of application, US have detected pancreatic pathology of great diversity. This article reviews the wide utility of US and the many examinations techniques, such as filling the stomach with water, changing the patient's position or suspending inspiration or expiration, allowing us to visualize all portions of the pancreas in a high percentage of patients.

Key words: Pancreas—Ultrasonography—Conventional imaging—Neoplasms—Inflammatory lesions—Pancreatic pseudocyst

Ultrasound imaging has made significant advances in recent years and plays an important role in the detection, characterization, and staging of pancreatic diseases. Conventional B-mode ultrasonography (US) is a noninvasive imaging modality that continues to be the first diagnostic step in the evaluation of the pancreas.

US can be considered the technique of choice in the initial evaluation of the pancreas. According to the long-standing literature, the pancreas can be visualized by US in a high percentage of patients [1]. Nevertheless, it is sometimes difficult to visualize the pancreatic area due to poor contrast between fat and pancreas.

The aims of this article are to describe the US appearance of the normal pancreas, the different US patterns detected in pancreatitis and its complications, and the US semiology of pancreatic neoplasms.

Technical background

The use of multifrequency transducers allows the study of the pancreas with the correct frequencies for any depth. Furthermore, new technologies improve pancreatic ultrasonographic imaging. Conventional imaging based not only on the amplitude information but also on the phase information of the return echo (Coherent Image Formation, Acuson, Siemens) for the formation of images, results in images with more information and greater detail resolution.

The image quality can also be improved by using compound technology. Compounding is a technology that reduces speckle in the B-mode image, thus improving contrast resolution and border detection (Fig. 1). Speckle is acoustic noise caused by the nature of US imaging. Compounding reduces speckle by generating several images or frames of data with independent information and then averaging these several frames of independent or partially independent information. There are different types of compounding technology available today, such as frequency compounding and spatial compounding (Fig. 1).

Another new technology that improves image quality because of the immediate identification of vascular structures is B-mode. This technology (Clarify Vascular Enhancement, Acuson, Siemens) optimizes the image by enhancing the B-mode display with information derived from power Doppler, clearly differentiating vascular anatomy from acoustic artifacts and surrounding tissue (Fig. 1).

The introduction of three-dimensional and four-dimensional technology opens new clinical possibilities for more complete evaluation of the pancreas in the future.

Correspondence to: A. Martínez-Noguera; email: amartinezno@santpau.es

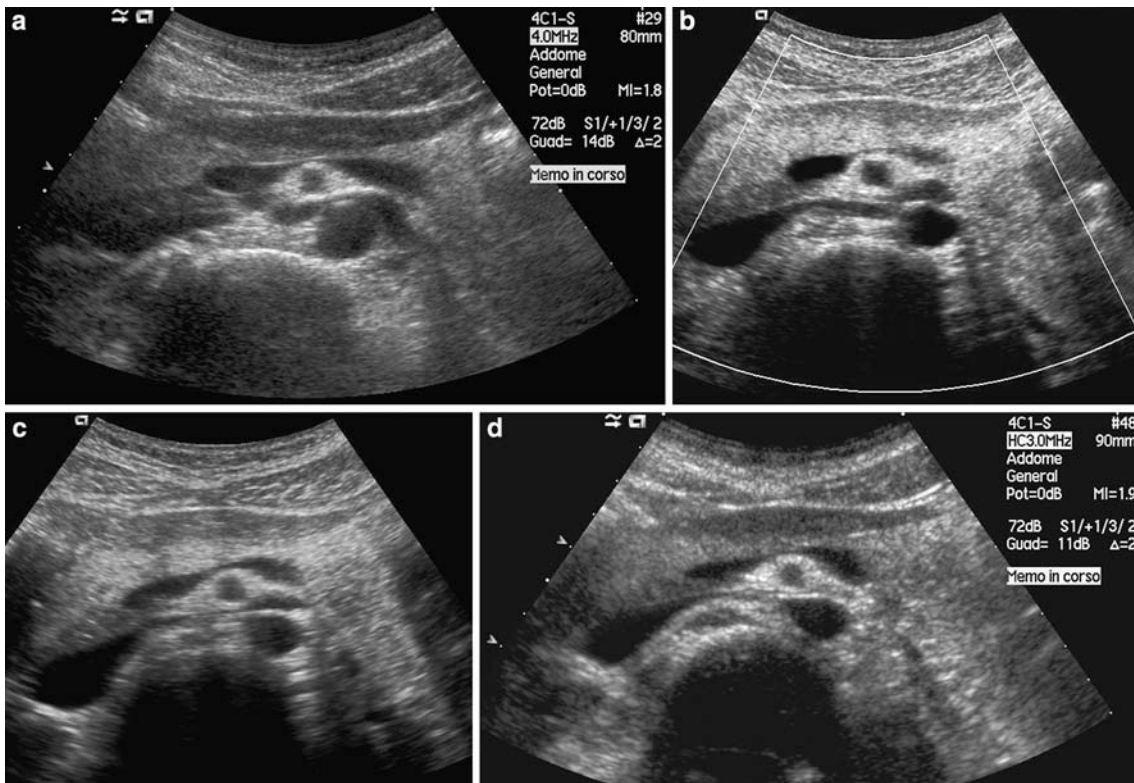


Fig. 1. Pancreas. **A** B-mode image (4.0 MHz). **B** Clarify Vascular Enhancement image (4.0 MHz). **C** Spatial Compound image (4.0 MHz). **D** Harmonic Compound image (3.0 MHz).

In general, the correct application of these new technologies in the study of the pancreas with US results in conventional imaging of the gland with very high spatial and contrast resolution (Fig. 1).

Examination protocols

In the study of the pancreas, US scan planes include transverse, longitudinal, and angled oblique scans. Bowel gas can be displaced by moving the transducer and applying compression when necessary. To obtain complete visualization of all the portions of the pancreatic gland it is possible and sometimes convenient to employ different scanning techniques, such as filling the stomach with water, examining the patient with suspended inspiration or expiration, and changing the patient's position to erect, supine, and left and right decubitus [1, 2].

US examination of the pancreas is performed following a minimum fast of 6 h. The purposes of the fast are to improve visualization of the pancreas, limit bowel gas, and ensure an empty stomach. Successful visualization of the pancreas is directly linked to the skill and persistence of the examiner. It is necessary to identify all portions of the pancreas—head, with the uncinate process, neck, body, and tail—in both the longitudinal and the transverse planes (Fig. 2). The pancreatic examination begins with the patient in the supine position. If the

pancreas is poorly visualized, the water technique is added, either alone or mixed with simethicone, which is an aqueous suspension that increases US transmission [3]. The patient is asked to drink 100 to 300 ml of water through a straw, in the erect or the left lateral decubitus position. The texture, size, and contour of the pancreas should always be evaluated. The echo pattern of the normal pancreas is isoechoic or hyperechoic compared to that of the normal liver (Fig. 2).

During US examination of the pancreatic gland it is very important to identify the main pancreatic duct (duct of Wirsung) but also the common bile duct, especially the intrapancreatic terminal tract. The splenic, superior mesenteric, and portal veins together with the celiac and superior mesenteric arteries must also be identified.

Normal anatomy

The pancreas arises from the fusion of two duodenal buds, dorsal and ventral. It is usually located at the level of the first or second lumbar vertebra; however, depending on the phase of respiration, it may be found at a slightly more caudal or cranial level. It has to be considered a quite fixed posterior organ.

The pancreas is usually divided into the head, with the uncinate process, neck, body, and tail regions. The uncinate process originates from the pancreatic head and lies posteriorly to the superior mesenteric vessels. The

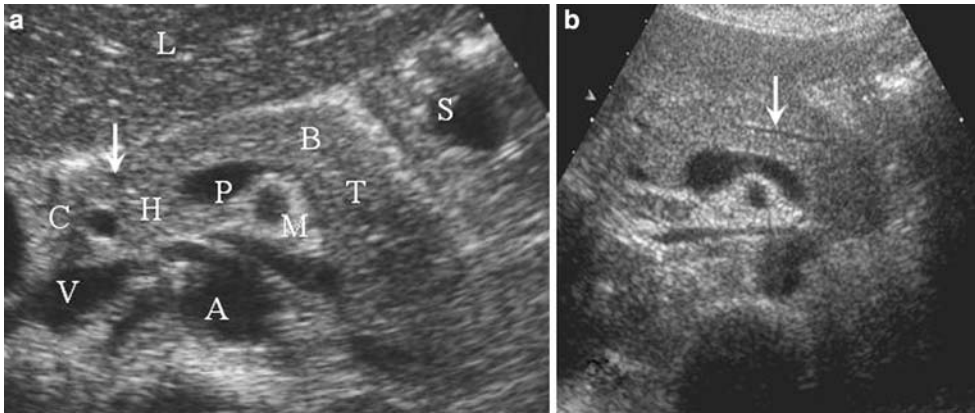


Fig. 2. Normal anatomy of the pancreas, vessels and landmarks. **A** Transverse US shows anatomical portions: H, head; B, body; T, tail. Vascular and ductal landmarks also seen in transverse US: A, aorta; V, cava; M, mesenteric

artery; P, portal vein (gastroduodenal artery [arrow]); C, common bile duct; S, stomach; L, liver. **B** Isoechoic pattern of the pancreatic gland in comparison to the left lobe of the liver; pancreatic duct (arrow).

anteroposterior dimensions of the pancreas vary greatly among individuals and tend to decrease with age. The following measurements are orientational: head, 2 cm; neck, < 1.0 cm; and body and tail, 1–2 cm [2].

Fatty replacement (lipomatosis) of the pancreas is a common finding with age, and in up to 35% of cases the gland may be as echogenic as the adjacent retroperitoneal fat [2, 4]. Complete fatty replacement is the most common pancreatic finding in patients with cystic fibrosis [5]. During US examination, structures surrounding the pancreas that may be misinterpreted as the gland are the third part of the duodenum, lymph nodes, and a papillary process of the caudate lobe [2, 6].

Vascular and ductal landmarks

The portal vein is formed behind the neck of the pancreas from the junction of the superior mesenteric and splenic veins. The superior mesenteric vein runs anteriorly to the uncinate process and posteriorly to the lower neck. The splenic vein runs from the splenic hilum along the posterior superior surface of the pancreas. The splenic artery arises from the celiac artery and runs along the superior margin of the gland, slightly anterior. The common hepatic artery arises from the celiac artery in 92% of patients [1]. It courses along the superior margin of the first portion of the duodenum and continues into the proper hepatic artery and gastroduodenal artery. The superior mesentery artery arises from the aorta behind the lower portion of the body of the pancreas and courses anteriorly to the uncinate process and to the third portion of the duodenum to enter the small bowel mesentery. The common bile duct crosses the anterior surface of the portal vein to the right of the proper hepatic artery. It goes behind the first portion of the duodenum to course inferiorly and posteriorly into the parenchyma of the head of the pancreas, where it is close

to the second portion of the duodenum. In the head of the pancreas, the internal diameter is no more than 4 mm [1].

The main pancreatic duct (duct of Wirsung) originates at the junction of the small ducts in the lobules of the tail. It is most frequently seen in the body and less frequently in the tail. It appears as a thin hypoechoic line bordered by two echogenic margins (Fig. 2). The upper limit of the main duct is 3 mm in young adults and 5 mm in the elderly. The secretin stimulation test increases duct size in 70%–100% of normal volunteers. This test could thus be helpful in the diagnosis of chronic pancreatitis and functional ductal obstruction [7].

Clinical application

Acute pancreatitis

Acute pancreatitis is an acute inflammatory process of the pancreas that may include suppuration, necrosis, and hemorrhage of pancreatic tissue, with variable involvement of other regional and remote tissues. Diagnosis is usually based on the laboratory assay of serum amylase and lipase levels. The most common causes are alcohol and cholelithiasis (70%); less common etiologies are postoperative, post-endoscopic retrograde cholangiopancreatography, abdominal trauma, drugs, and pregnancy (30%) [4]. Acute pancreatitis is classified as mild (interstitial edema) or severe (necrosis, fluid collections). Abdominal computed tomography (CT) is the technique of choice in the evaluation of patients who present clinical suspicion of pancreatitis. However, US is widely used. Biliary stones, peripancreatic collections, and pseudocysts can be detected. Normal US findings can be seen in patients with mild acute pancreatitis. In a large series, 14% of the patients did not show any significant CT findings [8]. Although the pancreas can appear normal in acute pancreatitis,

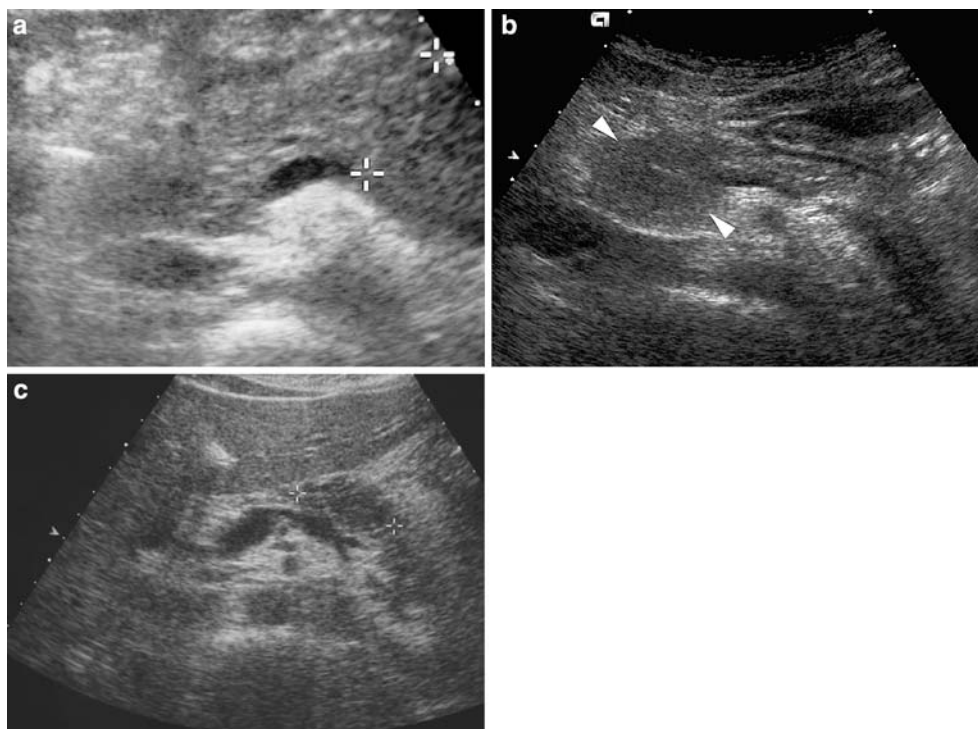


Fig. 3. Acute pancreatitis. **A** Transverse US with diffuse pancreatitis with a hypoechoic homogeneous pattern and global enlargement of the pancreas (*calipers*). **B** Focal acute pancreatitis of the pancreatic head (*arrowheads*) appearing at US with an enlarged pancreatic head slightly hypoechoic to the rest of parenchyma. **C** Focal acute pancreatitis of the pancreatic body. Transverse US with a hypoechoic area in the body–tail of the pancreas (*calipers*) in a patient with clinical findings not clearly indicating pancreatitis. A puncture was needed in this case.

the most frequent findings are enlargement of the gland and a diffuse decrease in normal echogenicity (Fig. 3). The pancreas is seen as more hypoechoic than the liver and the pancreatic texture may also appear heterogeneous. Acute pancreatitis can be focal or diffuse, depending on the distribution. Focal pancreatitis generally occurs in the pancreatic head and presents as a hypoechoic mass that is sometimes difficult to differentiate from a tumor, especially when focal acute pancreatitis occurs over chronic pancreatitis and the clinical findings are not clear or evident (Fig. 3) [9].

Complications of pancreatitis

Complications of acute pancreatitis include acute fluid collections, pseudocysts, pancreatic abscess, infected necrosis, and hemorrhage. Acute fluid collections occur in about 50% of patients, most commonly around the pancreas, in the anterior pararenal space and the lesser sac [10]. A pancreatic pseudocyst occurs in 40% of patients with acute pancreatitis and in 30% of patients with chronic pancreatitis. A pseudocyst is seen by US as a well-defined, anechoic structure with acoustic enhancement, and is typically round or oval (Fig. 4). Sometimes it may be septated, with internal echoes and inhomogeneous, thus simulating a cystic or necrotic solid tumor. Pseudocysts, however, are the most frequent cystic lesions of the pancreas [11]. To be sure of the diagnosis a history of severe acute pancreatitis or the morphologic changes of chronic pancreatitis must be present. The evidence of a well-visible wall of the pseudocyst can be related to the age of the lesion and

must be considered an important finding in therapeutic planning.

Pseudocysts can develop in 30% of patients, with extension into adjacent organs, hemorrhage, peritonitis, obstruction of the duodenum and bile ducts, and infection [2, 4, 11, 12]. In 50% of patients these cysts resolve spontaneously and in 20% they remain stable [2, 4, 12].

Abscesses consist of encapsulated collections of purulent material within or near the pancreas. They develop several weeks after the onset of pancreatitis. By US they are seen as an anechoic or heterogeneous mass containing bright echoes from pus, debris, or gas bubbles [13]. A pancreatic abscess should be suspected on the clinical evidence and when changes in the echogenicity of the content of pseudocysts are documented at US examination [13]. Pancreatic abscesses require percutaneous drainage or surgical debridement [14, 15]. Pancreatic phlegmons represent a combination of fat necrosis, tissue necrosis, extravasated pancreatic fluid, and, occasionally, hemorrhage. Differentiation from a pancreatic abscess is essential for appropriate clinical treatment.

Vascular complications including pseudoaneurysms and venous thrombosis may be seen in acute and chronic pancreatitis. Hemorrhage may occur as a consequence of vascular injury.

Chronic pancreatitis

Chronic pancreatitis is an inflammatory disease characterized by the replacement of the glandular elements of the pancreas by fibrous tissue. Chronic pancreatitis is



Fig. 4. Pseudocyst of the pancreas. Transverse US of the pancreas with a pseudocyst (*asterisk*) located in the pancreatic body.

clinically characterized by a progressive pancreatic functional loss. Common etiologies of chronic pancreatitis are alcohol, hyperlipidemia, hyperthyroidism, cystic fibrosis, and hereditary and idiopathic causes [16].

The diagnosis of chronic pancreatitis is based on clinical findings, laboratory evaluation of endocrine and exocrine pancreatic function, and imaging findings. Although early morphologic changes of chronic pancreatitis are difficult to recognize at imaging with different techniques, the findings of advanced disease are readily detected.

Alterations in the size of the pancreas may be seen in fewer than half of patients affected by chronic pancreatitis [7, 17, 18]. This percentage drops dramatically in the early stages of the disease. On the other hand, the finding of a gland of normal size does not exclude a diagnosis of chronic pancreatitis [17, 19]. Atrophy and focal alterations in size of the pancreas are more easily identified alterations (Fig. 5). However, these changes in pancreatic volume, although easily identifiable, are an expression of advanced stages of the disease in which the glandular contours appear irregular, sharp, and sometimes lumpy (Fig. 5). Echogenicity of the pancreas is usually increased in chronic pancreatitis due to adipose infiltration [20] and fibrosis [19, 21, 22]. Hyperechogenicity is not a specific parameter, however, also being present in elderly and obese subjects. Alteration of parenchymal echo structure, on the other hand, is a more specific sign of chronic pancreatitis. The pancreatic echotexture is inhomogeneous and coarse due to the coexistence of hyperechoic and hypoechoic foci (Fig. 6), foci of fibrosis and inflammation, respectively [19, 22]. These findings are described in 50%–70% of cases [17, 18]. In patients affected by severe exocrine pancreatic insufficiency, this percentage increases to about 80% [7], therefore showing the fairly good sensitivity of this finding. Apparent normality of the glandular echo

structure in chronic pancreatitis is reported in the literature in up to 40% of cases, and this is expected especially in the early stages of the disease [17, 23–25]. However, state-of-the-art US imaging has good capabilities for identifying the fine alterations of glandular texture present in the early stages of the disease, making the evaluation of pancreatic echostructural alterations an important finding for diagnosis. According to the Japan Pancreas Society [26], the most important diagnostic criterion for chronic pancreatitis is the presence of pancreatic calcifications (Fig. 5), whose identification is pathognomonic. Therefore, when there clinical suspicion of chronic pancreatitis, the presence of calcifications must always be accurately searched for. Pancreatic calcifications are calcium carbonate deposits, usually on a protein matrix (plugs) or on interstitial necrotic areas [17, 20, 27]. At US these appear as hyperechoic spots with a posterior shading, which may, however, be hardly detectable if the calcification is small (Fig. 5), due to the presence of artifacts from US beam refraction. The demonstration of pancreatic calcifications may be improved by the use of harmonic imaging and high-resolution US (Fig. 7) using a high US beam frequency and thus increasing US diagnostic accuracy [28]. Plugs with few or no calcium carbonate deposits, usually located in ducts, appear at US as echoic spots almost without posterior shading (Fig. 5). The high spatial and contrast resolution of state-of-the-art US systems technology allows, when there is an optimal view of the gland, accurate identification of pancreatic microcalcifications and microdeposits (Fig. 5).

Caliber abnormalities in chronic pancreatitis are essentially represented by main pancreatic duct dilation. Therefore the most significant US findings of chronic pancreatitis are pancreatic duct dilatation, intraductal calcifications, and pseudocysts.

According to some authors, the normal caliber should not be more than 2 mm when fasting [29, 30]. In the normal subject, however, the Wirsung duct caliber may be more than 2 mm in physiologic conditions such as postprandially [31]. The Wirsung duct must therefore be considered dilated when its caliber is larger than 3 mm [22]. In chronic pancreatitis, duct dilation is the most easily identified echographic sign (Fig. 5). Wirsung duct alterations have a sensitivity of about 60%–70% [18, 20] but, most importantly, a high specificity, about 80%–90% [18, 30, 32], for diagnosis. The limits of the reported sensitivity reflect the minor frequency of duct dilation in initial and/or light cases of chronic pancreatitis. In the early phases of chronic pancreatitis, the Wirsung duct may have a normal diameter [19]. Also, compression of the main pancreatic duct may lead to secondary obstructive chronic pancreatitis upstream of the obstacle with the same pathogenetic mechanism. Benign tumors, solid or cystic, and also pseudocysts may cause duct compression if

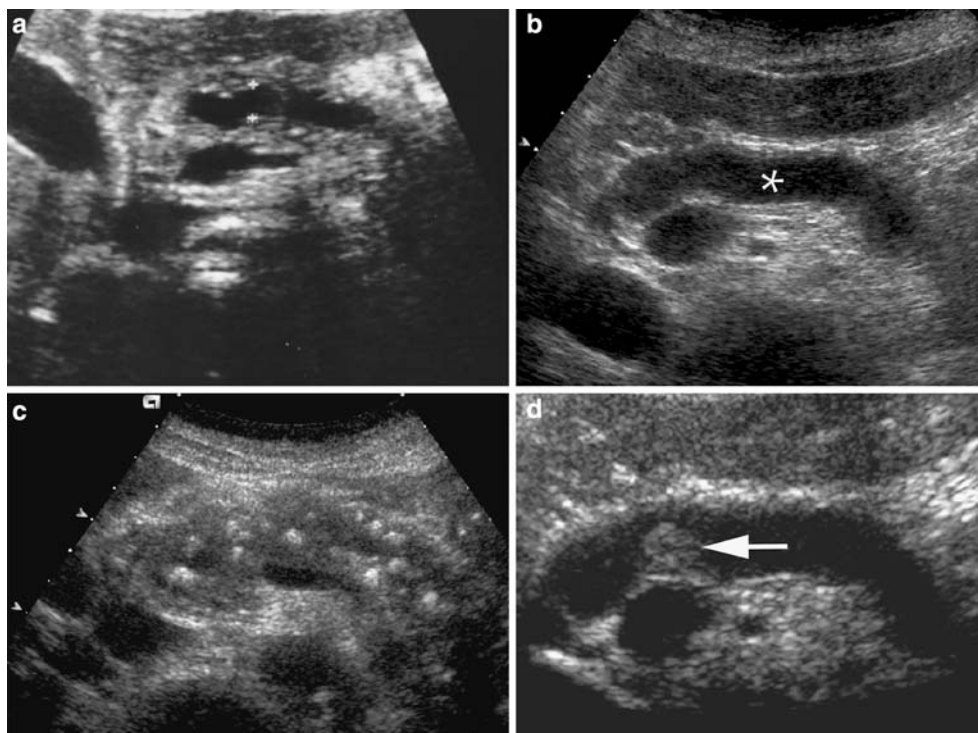


Fig. 5. Chronic pancreatitis. **A** Transverse US of the pancreas reveals duct dilatation (*calipers*) and moderate diffuse parenchyma atrophy. **B** Pancreatic atrophy in late-stage chronic pancreatitis. US shows a uniform dilatation of the Wirsung duct (*asterisk*) with important reduction of the pancreatic parenchyma. **C** US shows an increased volume of the pancreatic gland with an inhomogeneous echotexture owing to the presence of small calcifications, microcalcifications, and microdeposits. **D** The Wirsung duct is uniformly dilated with an endoluminal plug (*arrow*).

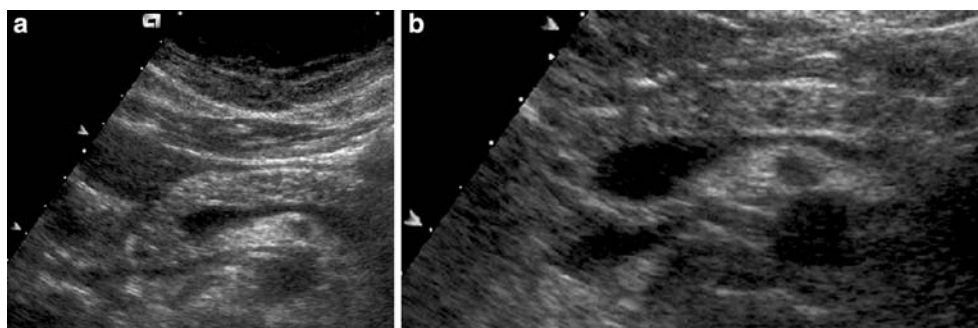


Fig. 6. Chronic pancreatitis. Ultrasonographic examination (**A**) shows an inhomogeneous and coarse echotexture of the pancreatic gland due to the coexistence of hyperechoic and hypoechoic foci in the parenchyma, better visible in the detailed image (**B**).

contiguous to the main pancreatic duct, with progressive development of obstructive chronic pancreatitis upstream [20].

Cystic dystrophy of the duodenal wall and groove pancreatitis occur in a border site (groove region) between the pancreas and the duodenum, which is difficult to access for a correct US evaluation. However, in the presence of Wirsung duct dilation *sine causa* at basal US (Fig. 8), the groove region should be examined with high-resolution US (Fig. 8). The use of high-frequency probes may better evaluate the proximal, juxtapancreatic, portions of the Wirsung duct (Fig. 8). Identification of small cystic formations in the thickened duodenal wall on the pancreatic side is a specific finding [32] for cystic dystrophy of the duodenal wall (Fig. 8).

Chronic pancreatitis may also manifest as a marked reduction in Wirsung duct caliber, as in autoimmune pancreatitis [34]. Because of the inflammation that may sometimes be segmental, especially in the initial stages,

these caliber alterations may be evident only in some parts of the pancreas. Wirsung duct contour alterations are US features of chronic pancreatitis that are more difficult to identify. Contour irregularity with alternation of frankly dilated and only ectatic tracts is typical of the advanced stages of chronic pancreatitis (Fig. 5). Ductal contour irregularity may, however, be found also upstream of a complete obstruction of the main pancreatic duct established in a short time, as for neoplastic infiltration (Fig. 9).

Intraductal calculi are protein aggregates with calcium carbonate deposits, which appear at US as round echoic particles, usually mobile. Intraductal protein matrix (plugs) echogenicity increases with the increase in their calcium content, until they become real intraductal calcifications (calculi) [19]. The mobility of intraductal calculi depends on the proportion between the ductal dilation and the diameter of the calculus itself. When possible, high-resolution US, by using a high US beam

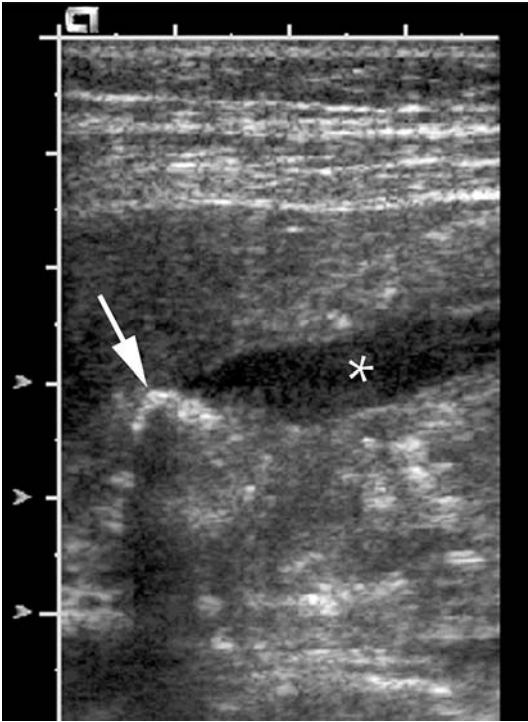


Fig. 7. Chronic pancreatitis. High-resolution US shows a small calcification (*arrow*) with well-visualized posterior shading inside the main pancreatic duct upstream dilated (*asterisk*).

frequency, may be useful for demonstration of their inclusions. High-resolution US improves the visualization of the angle that the deposit forms with the ductal wall (Fig. 7). Intraductal calculi must be considered as pathognomonic of chronic pancreatitis [26].

Focal pancreatitis has been reported to occur in 20% of cases and typically involves the pancreatic head [35]. Differentiation between pseudotumors in cases of chronic pancreatitis and pancreatic carcinoma may be difficult due to their similar patterns. Autoimmune chronic pancreatitis is a particular type of chronic pancreatitis, with a very recent pathological definition [34], caused by an autoimmune mechanism and related diseases such as primary sclerosing cholangitis and ulcerative colitis [36]. It is characterized by periductal inflammation, mainly substained by lymphocytic infiltration, with evolution to fibrosis [34]. As opposed to the other forms of chronic pancreatitis, the pancreas is increased in volume, usually in a diffused way with the typical “sausage” aspect, and the Wirsung duct is compressed or string-like [34]. US features include focal or diffuse pancreatic enlargement (Fig. 10), absence of any peripancreatic inflammation, fluid collection, and parenchymal calcification. US findings are characteristic in the diffuse form when the entire gland is involved (Fig. 10). Echogenicity is markedly reduced, gland volume is increased, and the Wirsung duct is compressed by glandular parenchyma, in which vessels are easily

demonstrated at color power Doppler US (Fig. 10). The differential diagnosis of focal forms of autoimmune chronic pancreatitis with ductal adenocarcinoma is a priority (Fig. 10).

The overall sensitivity of US in the diagnosis of chronic pancreatitis is variable, with an average range in most series of 60%–70% [7, 16]. After secretin stimulation in patients with chronic pancreatitis, the pancreatic duct presents no significant increase in caliber. Bolondi [7] reported an 87% sensitivity using this test with US. Complications of chronic pancreatitis are pseudocysts (30%), venous thrombosis (5%), malabsorption, and steatorrhea (50%) [4].

Pancreatic adenocarcinoma

About 90% of pancreatic tumors are ductal adenocarcinomas, and only 10% to 15% of patients are potentially resectable at the time of diagnosis. The major aims of imaging pancreatic malignancies are detection and staging, which determine the appropriate management options and ultimate prognosis of the disease. Tumors smaller than 1 cm and limited to the duct epithelium are considered early pancreatic duct adenocarcinoma [37, 38].

US is often the first technique performed when pancreatic adenocarcinoma is suspected. Pancreatic adenocarcinoma is most common in the pancreatic head (65%) and usually presents as a hypoechoic solid mass. General enlargement from associated pancreatitis is uncommon (15%). Masses in the head of the pancreas cause a ductal obstruction with secondary dilatation of both the common bile duct and the pancreatic duct (Fig. 9), resulting in the so-called double-duct sign. This presentation is, however, also common in the case of chronic pancreatitis. In particular aggressive forms of adenocarcinoma the development of necrosis or colliquation is common (Fig. 9). This is a process resulting from the difference between the growth rate and the formation of microvessels by angiogenesis. The necrotic/liquid part of the tumor is mainly located centrally (Fig. 9). A ductal adenocarcinoma is characterized by infiltrative margins with diffusion of the tumor in the adjacent parenchyma and structures. This feature could explain the common lack of clear-cut margins of this tumor during conventional US. As a result, the lesion can sometimes be difficult to identify or delineate (Fig. 11), especially if it is quite isoechoic to the adjacent pancreatic parenchyma. More frequently, however, the adenocarcinoma appears markedly hypoechoic to the adjacent pancreatic parenchyma. We argue that the ultrasound acoustic impedance of the ductal adenocarcinoma is very low. Moreover, sometimes the difference in impedance between the tumor and the pancreatic adjacent parenchyma is greater than the difference in beam attenuation at CT in both the pre- and the post-

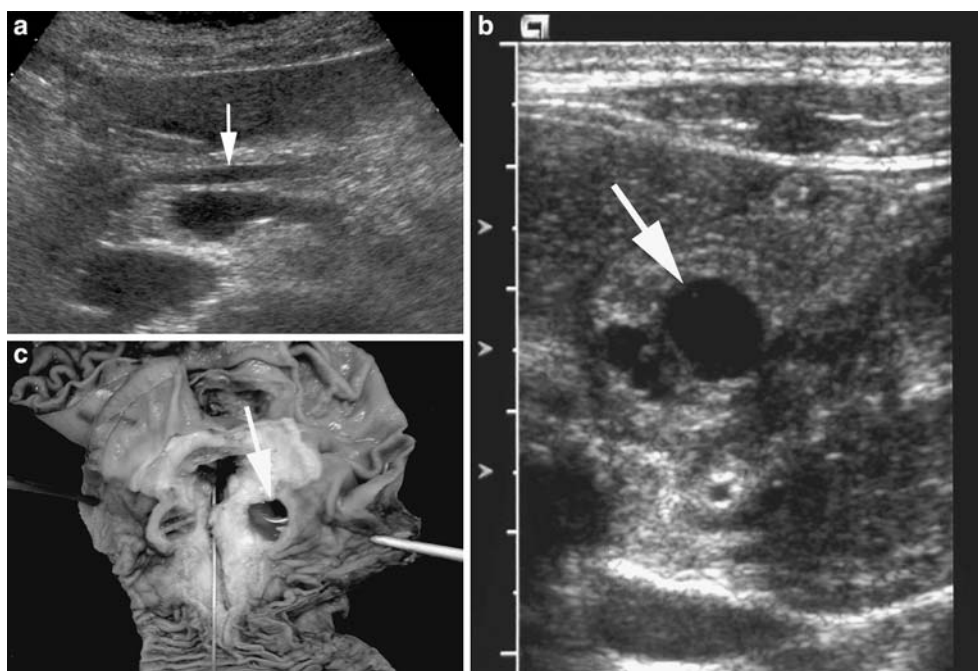


Fig. 8. Cystic dystrophy of the duodenal wall. **A** Ultrasonographic examination shows uniform dilation of the main pancreatic duct at the pancreatic body (*arrow*). **B** At high-resolution US very small cysts (*arrow*) are present in the “groove” region. **C** In the resected specimen the presence of small cysts (*arrow*) is diagnostic for cystic dystrophy of the duodenal wall.

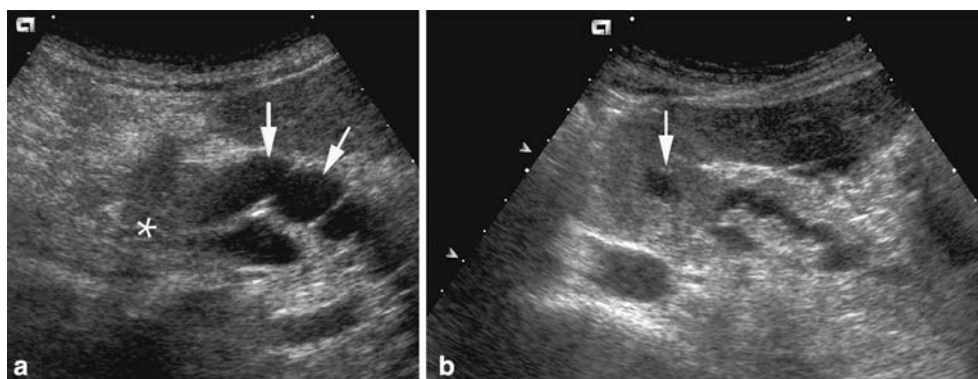


Fig. 9. Pancreatic adenocarcinoma. **A** Transverse US shows a hypoechoic mass in the pancreatic head (*asterisk*) with infiltration of the main pancreatic duct that is irregularly dilated upstream (*arrows*). **B** Hypoechoic mass in the pancreatic head with a small necrotic central area (*arrow*), with upstream dilation of the main pancreatic duct.

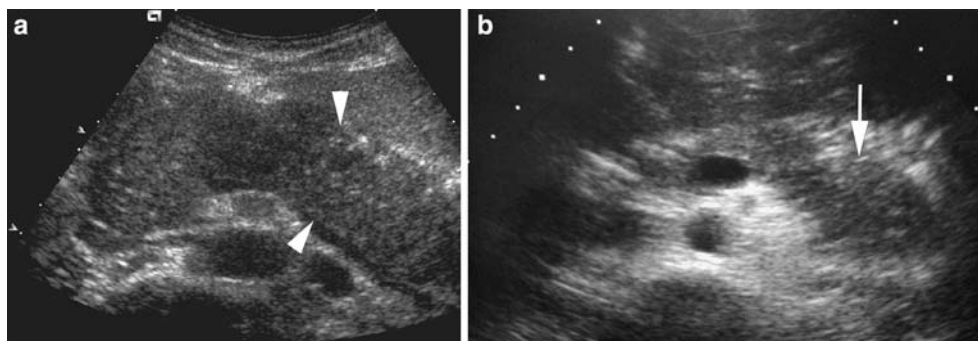


Fig. 10. Autoimmune pancreatitis. **A** Diffuse form. At ultrasound the pancreas is diffusely hypoechoic and increased in volume (*arrowheads*), with a “sausage” appearance. The Wirsung duct is completely compressed and not visible. **B** Focal form. Focal enlargement of the pancreatic tail (*arrow*) in a 25-year-old male without other radiological signs.

contrastographic phases (Fig. 12). This could explain some results reported in the literature on US identification of ductal adenocarcinoma [39].

The sensitivity of US tumor detection ranges from 72% to 98% and the specificity exceeds 90%, but even though some small pancreatic tumors are better resolved

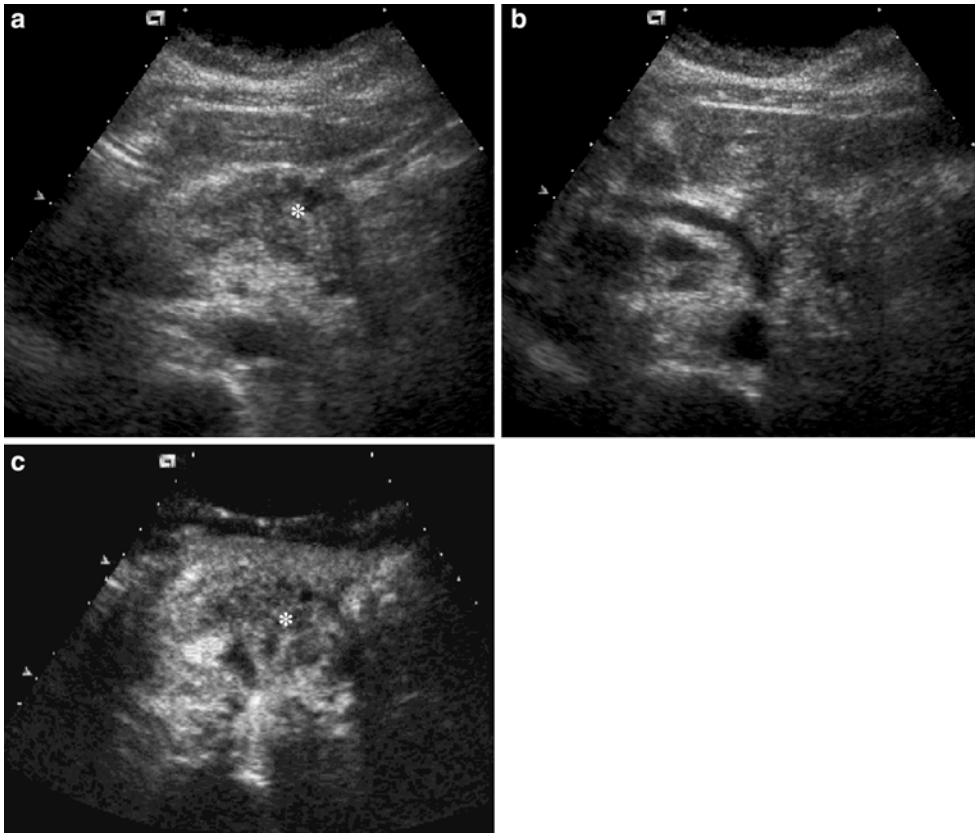


Fig. 11. Pancreatic adenocarcinoma. **A, B** Transverse US scans show an inhomogeneous, slightly enlarged pancreatic body (*asterisk*). **C** After contrast medium injection a hypoechoic mass (*asterisk*) involving the celiac artery is clearly visible.

by US than by CT (Fig.12), contrast-enhanced CT has a higher sensitivity than US [40, 41]. The integration of different imaging methods is sometimes necessary for tumor detection. Principal criteria for unresectable pancreatic cancer include liver or peritoneal metastases and invasion of major peripancreatic vessels.

Endocrine tumors

Pancreatic endocrine tumors or islet cell tumors arise from the neuroendocrine cells of the pancreas. These tumors are classified as functioning or nonfunctioning based on the presence or absence of symptoms related to hormone production. Insulinomas and gastrinomas are the most common functioning islet cell tumors and are usually small at the time of detection. Nonfunctioning tumors are frequently large at diagnosis and are often malignant [42]. The diagnosis is usually based on clinical and biochemical grounds. Diagnostic imaging is needed to localize the tumor and to study its relationship with vital structures for surgical resection.

Insulinomas are usually benign and solitary pancreatic lesions, while gastrinomas tend to be malignant and multiple. Insulinomas represent the most frequently found functioning neuroendocrine tumors of the pancreas (about 60% of all neuroendocrine tumors) and, in the majority of cases, are benign (85%–99%) and single (93%–98%) [43, 44]. Preoperative ultraso-

nographic detection of insulinomas is generally difficult but possible in 25%–60% of cases [45]. The ultrasonographic detection rate of insulinomas has increased steadily in the last 15 years [46–49], thanks to the increase in spatial, lateral, and contrast resolution provided by technological developments. The majority of insulinomas appear as hypoechoic pancreatic nodules, usually capsulated (Fig. 13). Sometimes very small calcifications can be present, especially in larger lesions [50].

At the time of clinical presentation 50% of the tumors are smaller than 1.5 cm [51]. When malignant, their diameter is generally > 3 cm, and about a third of these have metastases at the time of diagnosis [43, 44]. The mean diameter of insulinomas is < 15 mm, while gastrinomas are usually larger [50]. Abdominal US can detect only about 60% of isolated islet cell tumors.

Gastrinomas are the second most frequently found functioning neuroendocrine tumors of the pancreas (about 20% of all neuroendocrine tumors) [50, 51]. These tumors differ from insulinomas in localization, size, and vascularization [50, 52, 53]. They occur within the gastrinoma triangle (junction of the cystic duct and common bile duct–junction of the second and third parts of the duodenum–junction of the head and neck of the pancreas), of which only the pancreatic side is correctly explorable by US [51, 52]. Identification of pancreatic gastrinomas can be easy considering their

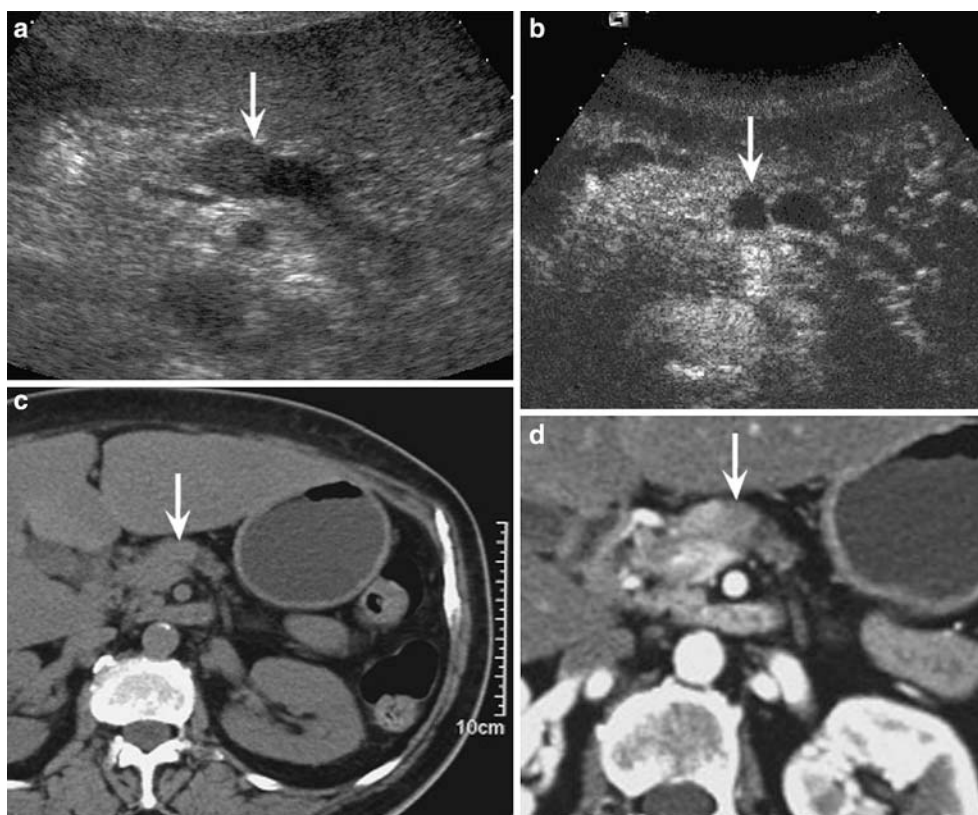


Fig. 12. Pancreatic adenocarcinoma. Transverse US scans **(A)** pre- and **(B)** post-contrast medium injection identify a small pancreatic adenocarcinoma (*arrow*) with good conspicuity with respect to the normal pancreatic parenchyma. CT scans **(C)** pre- and **(D)** post-contrast medium injection show the lesion (*arrow*) with less conspicuity than US examinations.

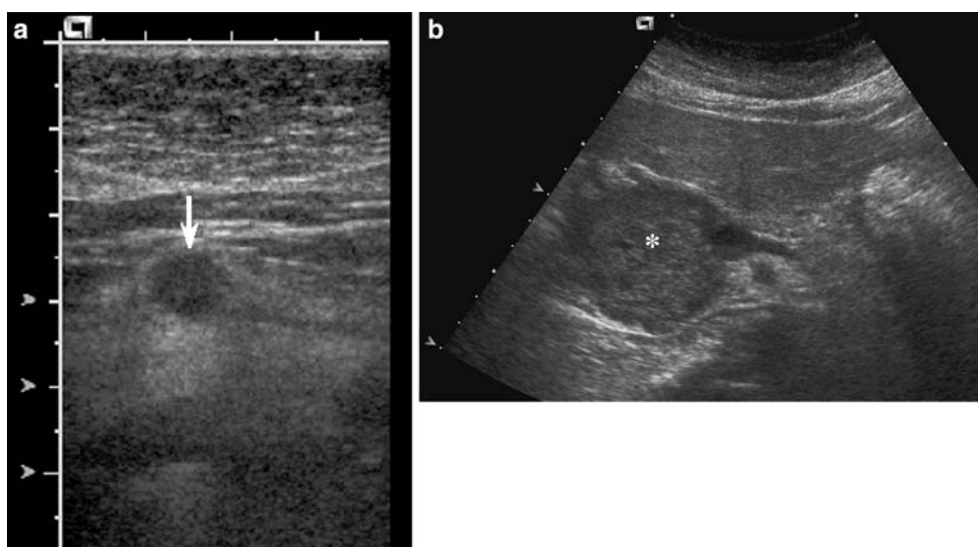


Fig. 13. Endocrine tumors. **A** Insulinoma. Transverse high-resolution US reveals a small hypoechoic lesion of <10 mm in the pancreatic body (*arrow*). **B** Nonfunctioning endocrine tumor. Transverse US shows a huge hypoechoic mass (*asterisk*), with well-defined margins, in the pancreatic head.

moderate size [52, 53]. Liver metastatic lesions are present in 60% of cases at the time of diagnosis [51, 54].

Nonfunctioning islet cell tumors represent up to 33% of neuroendocrine tumors of the pancreas [55], ranging from 1 to 20 cm in diameter and showing a high malignancy rate, up to 90% [55, 56]. They are, however, less aggressive than adenocarcinomas. The clinical presentation of nonfunctioning islet cell tumors is not

specific. These tumors, characterized by predominantly expansive growth, are not clinically apparent until adjacent viscera and structures have become involved. At US they appear well margined and usually easy to detect, thanks to their size (Fig. 13). Due to their dimensions, these tumors tend to necrosis and hemorrhage, developing a typical nonhomogeneous appearance, sometimes accompanied by very small intralesional calcifications. Larger nonfunctioning islet

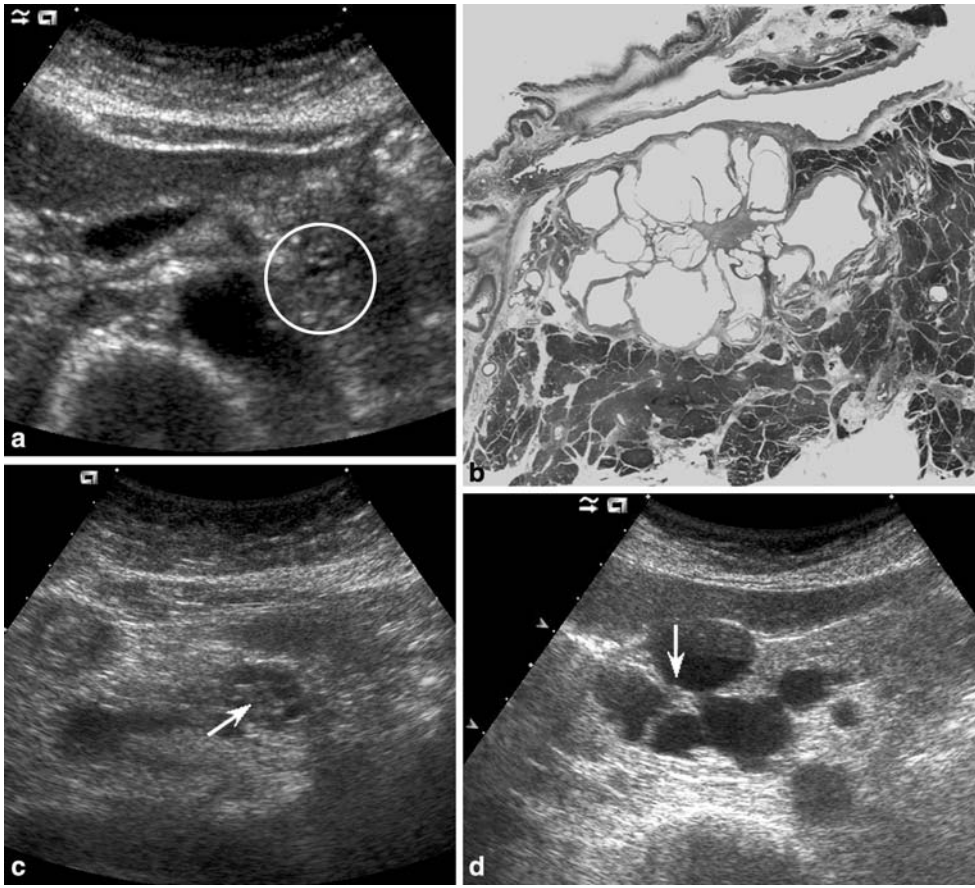


Fig. 14. Serous cystic tumors. **A** Very small microcystic lesion (*circled*) in the pancreatic body. **B** Macroscopic sponge aspect of the serous cystadenoma. **C, D** Transverse US demonstrates the central scar as the central, solid, echogenic portion of the lesion (*arrow*) in two serous cystadenomas located (C) in the pancreatic body and (D) in the pancreatic head.

cell tumors show cystic degeneration or cystic change [50]. Inside the lesion a well-organized relationship exists between neoplastic cells and neovessels traveling into the tumoral stroma [42]. This is responsible for the hypervascular nature of the lesion. For this reason, characterization of these tumors depends on the demonstration of their hypervascularization [50, 57].

The other functioning neuroendocrine tumors (vipoma, glucagonoma, and somatostatinoma) are more rare; all together they account for about 20% of functioning neuroendocrine tumors of the pancreas [50, 51].

Cystic pancreatic tumors

Cystic pancreatic tumors are uncommon and represent only 10%–15% of all pancreatic tumors [4]. The most common types of cystic neoplasms of the pancreas include serous and mucinous tumors. The differential diagnosis of cystic pancreatic lesions is important in relation to different etiologies (pseudocysts, tumors) and prognosis (benign, malignant). The differential diagnosis includes congenital true cysts and acquired cysts (pseudocysts, hydatid cysts, cystic neoplasms) [58].

Serous cystadenoma (SCA) is a benign lesion and has a strong female predilection after the sixth decade of life.

It is usually located in the head of the pancreas and generally characterized by tiny cysts [11] of <20 mm (Fig. 14). The content of the cysts is a glycogen-rich serous fluid that is transonic at US. The serous cystadenoma, when extremely microcystic, can have a solid appearance at US and CT. In up to 15% of cases, the tumor contains a central scar, which may calcify. US imaging can show the microcystic appearance of this lesion related to the sponge macroscopic aspect (Fig. 14). The central scar, when present, is often visible as the central solid echogenic portion of the tumor (Fig. 14), sometimes containing calcifications (Fig. 14). It is very important to depict at US other typical features of SCA that may suggest the diagnosis. The contours of the SCA are always quite sinuous and the wall is thin. The internal septa of SCA normally are well orientated and centrally directed, reaching the central scar with a definitive typical aspect of the skeleton of this cystic lesion. Numerous thin septa with a radial arrangement give the lesion its typical microcystic aspect.

SCAs do not communicate with the main pancreatic duct. The demonstration of this is fundamental, especially when the lesion is large, because it might compress the main pancreatic duct that is a upstream dilated. Demonstration of the absence of communication, however, is impossible by US and is a specific issue for

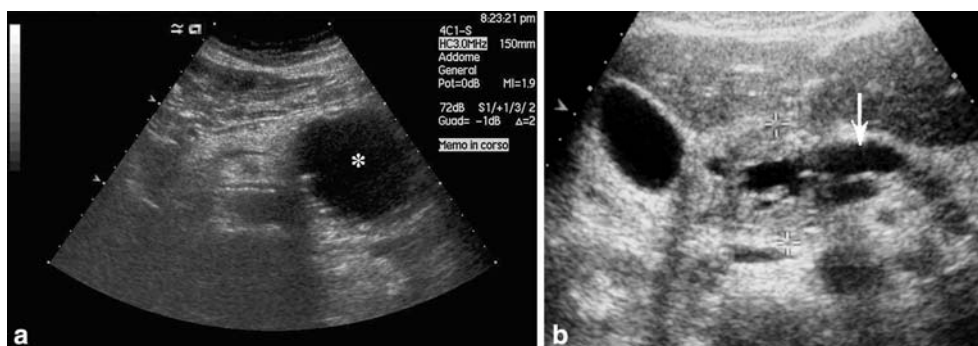


Fig. 15. Mucinous cystic tumors. **A** Mucinous cystadenoma. A large cystic lesion of the pancreatic body (*asterisk*) with a thick irregular wall containing very small hyperechoic calcifications. **B** Localized main duct type of IPMT. US shows a highly inhomogeneous mass (*calipers*) with upstream dilation of the main pancreatic duct (*arrow*).

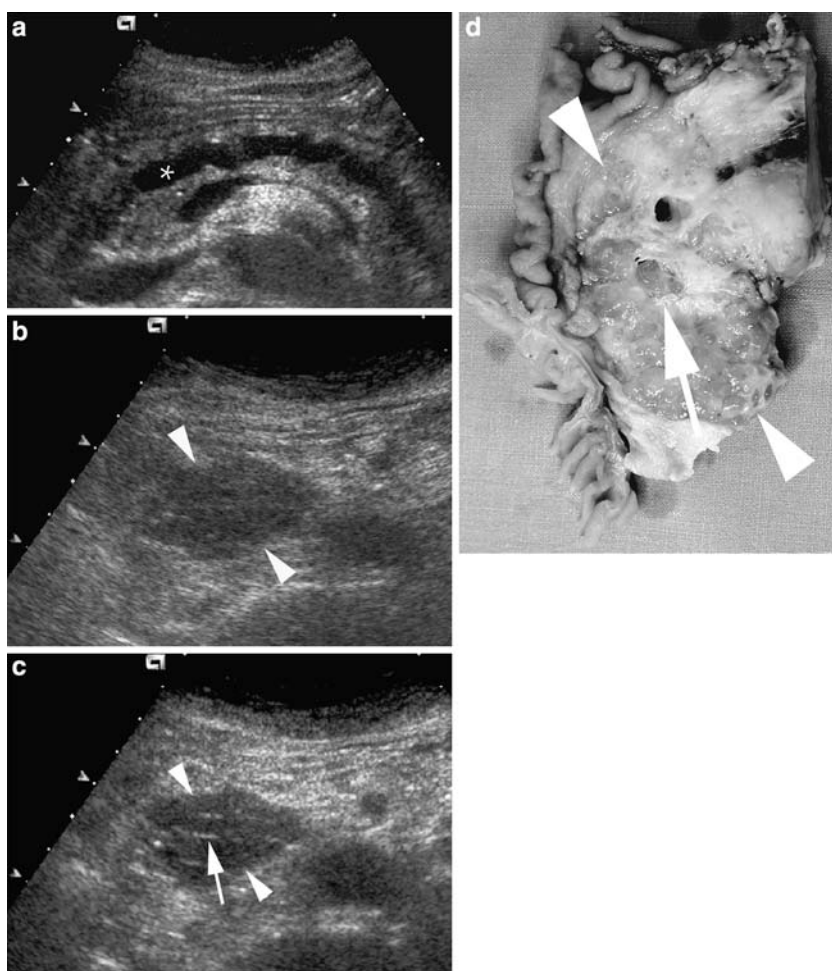


Fig. 16. Branch duct-type IPMT of the uncinus process of the pancreas. Ultrasonographic examination shows **(A)** dilation of the main pancreatic duct at the pancreatic body (*asterisk*) and **(B)** a hypoechoic mass at the uncinus process of the pancreas (*arrowheads*). **C** At ultrasonographic harmonic imaging, more or less sharp intralésional interfaces (*arrow*) become visible inside the hypoechoic lesion (*arrowheads*). **D** In the resected specimen (*arrowheads*) very small intralésional septa (*arrow*) are visible.

magnetic resonance imaging (MRI) and endoscopic retrograde cholangiopancreatography. Differential diagnosis between serous and mucinous cystic tumors is a fundamental issue of imaging considering the different management required for these two lesions, so as to avoid aggressive surgical intervention for SCAs [58]. SCA, being a benign lesion, can be followed up.

Mucinous cystic neoplasm is a malignant or potentially malignant lesion. It is more common in women in their fourth to sixth decade and it is most often located in the body or tail of the pancreas. The mucinous cystic tumor is extremely peripherally located in the pancreatic parenchyma and shows cysts that are less numerous and larger in size than typically seen with SCA. The content

of the cyst is mucin. At US, a mucinous cystic neoplasm appears as round to ovoid, with unilocular or multilocular cystic lesions, each >20 mm. Mucinous cystic tumors are characterized by the presence of thick walls and, occasionally, peripheral calcifications (Fig. 15). The mucinous content is viscous and may generate fine echoes in the internal part of the lesion that covers the internal wall of the cystic tumor and may have the inclusion such as internal septa and/or solid papillary projections. Demonstration of these inclusions, and if possible of their vascularization, is fundamental for the diagnosis. The number and the thickness of intralésional septa and nodules are not always related to the grade of malignancy. Mucinous tumors may spread, involve lymph nodes, and produce liver metastases [5, 60].

Intraductal papillary mucinous tumor (IPMT) is recognized as a dilatation of the main pancreatic duct and/or its branches or cyst formation with proliferation of pancreatic ductal epithelium and excessive production of mucin. IPMTs are classified into the main duct type, branch duct type, or a combination of the two [61]. The main duct type can be localized or diffuse. The localized main duct type of IPMT is characterized by highly inhomogeneous masses, related to neoplastic intraductal proliferation, with upstream dilatation of the main pancreatic duct (Fig. 15). The diffuse main type may be difficult to distinguish from chronic pancreatitis. The branch duct mucinous tumor is characterized by cystic ectasia of the branch, forming a mass. At US examination the mucin of IPMT, especially the ductectatic mucin-hypersecreting variant of the branch ducts, may not be easily differentiated from the solid portions of the tumor, which can therefore be mistakenly reported as solid (Fig. 16). Harmonic imaging, with its better contrast resolution [62, 63], may lead to identification of the part of the IPMT that is not solid, thanks to the demonstration of more or less sharp intralésional interfaces (Fig. 16). However, with US, final diagnosis of IPMT by demonstration of the communication between the tumor and the pancreatic duct is difficult [64]. These tumors have a better prognosis than pancreatic adenocarcinomas. MRI may better show the cystic dilatation of branch ducts as well as nodules and septa inside the cystic lesion [65].

Lymphoma and metastases

Pancreatic lymphoma is represented by the non-Hodgkin B-cell histotype, and in the majority of cases it is associated with lymph nodes or lesions in other organs. US shows focal or diffuse pancreatic enlargement that is hypoechoic to normal pancreatic parenchyma. Diffuse pancreatic enlargement may be due to a diffuse pancreatic tumor or pancreatitis associated with tumor.

Primary tumors that most frequently metastasize to the pancreas are from the lung, breast, kidney, or melanoma [66]. Pancreatic metastases can appear as focal, multifocal lesions or diffuse enlargement of the pancreas in a patient with a known primary neoplasm.

New trends and developments

Although conventional US has proved its value in the majority of pancreatic diseases, a number of technological improvements have been introduced in the last decade that have increased the accuracy of this method: these include tissue harmonic imaging and, more recently, contrast-enhanced US. These advances in imaging are discussed in the subsequent papers of this feature section.

References

- Mittelstaedt CA (1987) *Abdominal ultrasound*. New York: Mosby, pp 163–176
- Rumack C, Wilson SR, Charboneau JW (1991) *Diagnostic ultrasound*. New York: Mosby Year Book, pp 145–177
- Lev-Toaff AS, Bree RL, Lund PJ, Saini S, Bluth EI, Goldberg BB (1998) Use of simethicone-coated cellulose suspension to improve pancreatic ultrasound: experience in 55 patients with pancreatic pathology. *Radiology* 209 (Suppl):310
- Weissleder R, Rieumont MJ, Wittenberg J (1997) *Primer of diagnostic imaging*. 2nd ed. New York: Mosby Year Book, pp 220–228
- Tham RT, Heyerman HG, Falke TH, et al. (1991) Cystic fibrosis: MR imaging of the pancreas. *Radiology* 179:183–186
- Donoso L, Martínez-Noguera A, Zidan A, et al. (1989) Papillary process of the caudate lobe of the liver: sonographic appearance. *Radiology* 173:631–633
- Bolondi L (1989) Sonography of chronic pancreatitis. *Radiol Clin North Am* 27:815–833
- Balthazar EJ, Ranson JHC, Naidich DP, et al. (1985) Acute pancreatitis: prognostic value of CT. *Radiology* 156:767–772
- Lorén I, Lasso A, Fork T, et al. (1999) New sonographic imaging observations in focal pancreatitis. *Eur Radiol* 9:862–867
- Baron HT, Morgan ED (1997) The diagnosis and management of fluid collections associated with pancreatitis. *Am J Med* 102:555–563
- Procacci C (2001) Pancreatic neoplasms and tumor-like conditions. *Eur Radiol* 11(Suppl 2):S167–S192
- Kourtesis G, Wilson S, Williams R (1990) The clinical significance of fluid collections in acute pancreatitis. *Am Surg* 56:796–799
- Procacci C, Mansueto G, D'Onofrio M, et al. (2002) Non-traumatic abdominal emergencies: imaging and intervention in acute pancreatic conditions. *Eur Radiol* 12(10):2407–2434
- Balthazar EJ, Freeny PC, Van Sonnenberg E (1994) Imaging and intervention in acute pancreatitis. *Radiology* 193:297–306
- Ranson J, Rifkind R, Roses D (1975) Prognostic signs and role of operative management in acute pancreatitis. *Surg Gynecol Obstet* 139:69–80
- Freeny P, Lawson T (1982) *Radiology of the pancreas*. New York: Springer-Verlag, p 449
- Alpern MB, Sandler MA, Kellman GM, Madrazo BL (1985) Chronic pancreatitis: ultrasonic features. *Radiology* 155:215–219
- Bolondi L, Priori P, Gullo L, et al. (1987) Relationship between morphological changes detected by ultrasonography and pancreatic esocrine function in chronic pancreatitis. *Pancreas* 2:222–229
- Lecesne R, Laurent F, Drouillard J, et al. (1999) Chronic pancreatitis. In: Baert AL, Delorme G, Hoe L Van (eds) *Radiology of the pancreas*. 2nd rev ed. New York: Springer Verlag, pp 145–180
- Lankisch PG, Banks PA (1998) Chronic pancreatitis: etiology. In: Lankisch PG, Banks PA (eds) *Pancreatitis*. New York: Springer Verlag, pp 199–208

21. Husband JE, Meire HB, Kreel L (1977) Comparison of ultrasound and computer tomography in pancreatic diagnosis. *Br J Radiol* 50:855–863
22. Remer EM, Baker MB (2002) Imaging of chronic pancreatitis. *Radiol Clin N Am* 40:1229–1242
23. Lees WR, Vallon AD, Denyer ME, et al. (1979) Prospective study of ultrasonography in chronic pancreatic disease. *BMJ* 1:162–164
24. Foley WD, Stewart ET, Lawson TL, et al. (1980) Computer tomography, ultrasonography and echoscopic retrograde cholangiopancreatography in the diagnosis of pancreatic disease: a comparative study. *Gastrointestinal Radiol* 5:29–35
25. Grant TH, Efrusy ME (1981) Ultrasound in the evaluation of chronic pancreatitis. *JAMA* 81:183–188
26. Homma T, Harada H, Koizumi M (1997) Diagnostic criteria for chronic pancreatitis by the Japan Pancreas Society. *Pancreas* 15:14–15
27. Ring EJ, Eaton SB, Ferrucci JT, Short WF (1973) Differential diagnosis of pancreatic calcification. *Am J Roentgenol Radium Ther Nucl Med* 117:446–452
28. Balthazar EJ (1994) Pancreatitis. In: Gore RM, Levine MS, Laufer I (eds) *Textbook of gastrointestinal radiology*. Philadelphia: WB Saunders, pp 2132–2160
29. Lawson TL, Berland LL, Foley WD, et al. (1982) Ultrasonic visualization of the pancreatic duct. *Radiology* 144:865–871
30. Niederau C, Grendell JH (1985) Diagnosis of chronic pancreatitis. *Gastroenterology* 88:1973–1995
31. Brogna A, Bucceri AM, Catalano F, et al. (1991) Ultrasonographic study of the Wirsung duct caliber after meal. *Ital J Gastroenterol* 23:208–210
32. Hessel ST, Siegelman SS, McNeil BJ, et al. (1982) A prospective evaluation of computer tomography and ultrasound of the pancreas. *Radiology* 143:129–133
33. Procacci C, Graziani R, Zamboni G, et al. (1997) Cystic dystrophy of the duodenal wall: radiologic findings. *Radiology* 205:741–747
34. Furukawa N, Muranaka T, Yasumori K, et al. (1998) Autoimmune pancreatitis: radiologic findings in three histologically proven cases. *J Comput Assist Tomogr* 22:880–883
35. Neff CC, Simeone JF, Witenberg J, et al. (1984) Inflammatory pancreatic masses. Problems in differentiating focal pancreatitis from carcinoma. *Radiology* 150:35–38
36. Irie H, Honda H, Baba S, et al. (1998) Autoimmune pancreatitis: CT and MR characteristics. *AJR* 170:1323–1327
37. Rosewicz S, Wiedenman B (1997) Pancreatic carcinoma. *Lancet* 349:485–489
38. Ichikawa T, Haradome H, Hachiya J, et al. (1997) Pancreatic ductal adenocarcinoma: preoperative assessment with helical CT versus dynamic MR imaging. *Radiology* 202:655–662
39. Minniti S, Bruno C, Biasiutti C, et al. (2003) Sonography versus helical CT in identification and staging of pancreatic ductal adenocarcinoma. *J Clin Ultrasound* 31(4):175–182
40. Niederau C, Grendell JH (1992) Diagnostic of pancreatic carcinoma: imaging techniques and tumor markers. *Pancreas* 7:66–86
41. Karlson BM, Ekbohm A, Lindgren PG, et al. (1999) Abdominal US for diagnosis of pancreatic tumor: prospective cohort analysis. *Radiology* 213:107–111
42. Buetow PC, Miller DL, Parrino TV (1997) Islet cell tumors of the pancreas: clinical, radiologic, and pathologic correlation in diagnosis and localization. *Radiographics* 17:453–472
43. Liu TH, Tseng HC, Zhu Y (1985) Insulinoma. An immunohistochemical and morphologic analysis of 95 cases. *Cancer* 56:1420–1429
44. Stefanini P, Carbonni M, Patrassi N (1974) Beta islet-cell tumors of the pancreas: result of a study on 1067 cases. *Surgery* 75:597
45. Galiber AK, Reading CC, Charboneau JW (1988) Localization of pancreatic insulinoma: comparison of pre- and intraoperative ultrasound with computer tomography and angiography. *Radiology* 166(2):405–408
46. Shawker TH, Doppman JL, Dunnick NR, McCarthy DM (1982) Ultrasonic investigation of pancreatic islet cell tumors. *J Ultrasound Med* 1(5):193–200
47. Gianello P, Gigot JF, Berthet F, et al. (1988) Pre- and intraoperative localization of insulinomas: report of 22 observations. *World J Surg* 12(3):389–397
48. Van Hoe L, Gryspeerdt S, Marchal G, et al. (1995) Helical CT for the preoperative localization of islet cell tumors of the pancreas: value of arterial and parenchymal phase images. *AJR* 165(6):1437–1439
49. Angeli E, Vanzulli A, Castrucci M, et al. (1997) Value of abdominal sonography and MR imaging at 0.5 T in preoperative detection of pancreatic insulinoma: a comparison with dynamic CT and angiography. *Abdom Imaging* 22(3):295–303
50. D'Onofrio M, Mansueto GC, Falconi M, Procacci C (2004) Neuroendocrine pancreatic tumor: value of contrast enhanced ultrasonography. *Abdom Imaging* 29:246–258
51. Ros PR, Morteale KJ (2001) Imaging features of pancreatic neoplasms. *JBR-BTR* 84(6):239–249
52. Pereira PL, Wiskirchen J (2003) Morphological and functional investigations of neuroendocrine tumors of the pancreas. *Eur Radiol* 13(9):2133–2146
53. Semelka RC, Cumming MJ, Shoenut JP, Magro, et al. (1993) Islet cell tumors: comparison of dynamic contrast-enhanced CT and MR imaging with dynamic gadolinium enhancement and fat suppression. *Radiology* 186(3):799–802
54. Mergo PJ, Helmberger TK, Buetow PC, et al. (1997) Pancreatic neoplasm: MR imaging and pathologic correlation. *Radiographics* 17:281–301
55. Fugazzola C, Procacci C, Bergamo Andreis IA, Iacono C, et al. (1990) The contribution of ultrasonography and computed tomography in the diagnosis of nonfunctioning islet cell tumors of the pancreas. *Gastrointest Radiol* 15(2):139–144
56. Eckhauser FE, Cheung PS, Vinik AI, et al. (1986) Nonfunctioning malignant neuroendocrine tumors of the pancreas. *Surgery* 100:978–988
57. Procacci C, Carbognin G, Accordini S, et al. (2001) Nonfunctioning endocrine tumors of the pancreas: possibilities of spiral CT characterization. *Eur Radiol* 11:1175–1183
58. Yeo CJ, Sarr MG (1994) Cystic and pseudocystic diseases of the pancreas. *Curr Probl Surg* 31:165–243
59. Kalra MK, Maher MM, Sahani DV, et al. (2002) Current status of imaging in pancreatic diseases. *J Comput Assist Tomogr* 26:661–675
60. Ros PR, Hamrick-Turner JE, Chiechi MV, et al. (1992) Cystic masses of the pancreas. *Radiographics* 12:673–686
61. Procacci C, Megibow AJ, Carbognin G, et al. (1999) Intraductal papillary mucinous tumor of the pancreas: a pictorial essay. *Radiographics* 19:1447–1463
62. Shapiro RS, Wagreich J, Parsons RB, et al. (1998) Tissue harmonic imaging sonography: evaluation of image quality compared with conventional sonography. *AJR* 171:1203–1206
63. Bennett GL, Hann LE (2001) Pancreatic ultrasonography. *Surg Clin North Am* 81:259–281
64. Procacci C, Schenal G, Dalla Chiara E, et al. (2003) Intraductal papillary mucinous tumors: imaging. In: Procacci C, Megibow AJ (eds) *Imaging of the pancreas cystic and rare tumors*. Berlin: Springer Verlag, pp 97–137
65. Keppke AL, Miller FH (2005) Magnetic resonance imaging of the pancreas: the future is now. *Semin Ultrasound CT MRI* 26:132–152
66. Merkle EM, Braz T, Kolkythas O, et al. (1998) Metastases to the pancreas. *Br J Radiol* 71:1208–1214